Letter
Vol. 48, No. 1 / 1 January 2023 / Optics Letters 179

Optics Letters

Desensitization design method of a freeform optical system based on local curve control

Zichang Qin,[1,2] Qingyu Meng,[1,*] and Xiaodong Wang[1]

[1] Changchun Institute of Optics, Fine Mechanics and Physics, Chinese Academy of Sciences, Jilin, Changchun 130033, China
[2] University of the Chinese Academy of Sciences, Beijing 100049, China
*Corresponding author: mengqy@ciomp.ac.cn

Received 11 November 2022; revised 25 November 2022; accepted 25 November 2022; posted 28 November 2022; published 23 December 2022

In this Letter, an error sensitivity evaluation function of freeform optical systems is proposed, and a desensitization design method is established. This method adopts the idea of micro-elements and, based on geometric optics theory, studies the relationship between the local curve of the freeform surface and the change of the wavefront error (Δ*WE*) when the optical system is disturbed by the position error, and realizes the desensitization design of the optical system. By simply changing the evaluation function, the method can be applied to the desensitization design of any optical system with any surface (spherical, aspheric, and freeform surface).

https://doi.org/10.1364/OL.480641

With their higher degrees of freedom, freeform surfaces perform well in aberration correction and have been applied in many fields [1–5]. However, most of the current studies still focus on the design of optical systems with higher performance, without considering the as-built performance of these systems [6–8]. How to optimize the imaging quality of freeform surface optical systems while reducing the error sensitivity is the subject of this Letter.

At present, there are two methods of optimizing freeform optical systems. One is to adopt error sensitivity optimization methods applicable to all optical systems, such as the global search method [9,10], the multiple structure optimization method [8], or optical design software's built-in desensitization optimization method. This method does not explore the principle, but only focuses on the results. In order to obtain ideal optimization results, tolerance analysis and as-built performance evaluation on a large number of systems must be carried out, which consumes a lot of calculation and optimization time. Another way is to use a variety of desensitization design methods to optimize the spherical or conic optical system. After obtaining an ideal initial structure of the freeform optical system, the surface is upgraded to a freeform surface to further optimize the imaging quality and error sensitivity [11,12]. This method requires designers to have a lot of experience so that they can modify the error sensitivity evaluation function to be suitable for the optimization process of freeform optical systems. At present, there is no optimal design method of freeform surface optical systems that considers image quality optimization and error sensitivity optimization at the same time.

In this Letter, we propose a new method to evaluate and optimize the error sensitivity of freeform surface optical systems based on local curvature (LC) control. This method uses the idea of micro-elements to decompose the complex freeform surface into several simple conic surfaces. By controlling the LC of the optical element, the change of wavefront error (ΔWE) caused by the error of the optical system is reduced to lower the error sensitivity. This method is suitable for evaluating all smooth and continuous freeform surfaces. With a focal length of 850 mm, F# 4.25, and field of view (FOV) of 20°×30°, the off-axis three-mirror optical system working at 588 nm is taken as an example to optimize the design of desensitization . Through the Monte Carlo tolerance analysis method, compared with the traditional design method and Zemax OpticStudio's built-in "TOLR" method, the results obtained by the desensitization design method proposed by us have less ΔWE and shorter optimization time under the same error conditions, which validates the research content and the effectiveness of the desensitization design method.

In this Letter, with the two most representative error types (tilt and decenter) as examples, the relationship between ΔWE and the optical system parameters is explored when the optical system generates error disturbances by means of ray tracing. Furthermore, the core of error sensitivity of the optical system is obtained, and the desensitization design method is established.

The mathematical analysis model of the error sensitivity of the single mirror reflective optical system is shown in Fig. 1. The black curve represents the mirror, and the center of the mirror intersects with the optical axis at point O. The green dashed curve represents the mirror with tilt, and the light blue dashed curve represents the mirror with decenter. The incidence light intersects with the mirror at point A, and the reflected ray intersects with the optical axis at point B. When the mirror applied tilt error, the tilt angle is α, as shown in Fig. 1(a). The incidence ray intersects with the mirror at A_t, and the reflected ray intersects with the optical axis at point B_t. When the decenter error is applied to the mirror, the decenter error is Δh, as shown in Fig. 1(b). The incidence ray intersects with the mirror at A_d, and the reflected ray intersects with the optical axis at B_d.

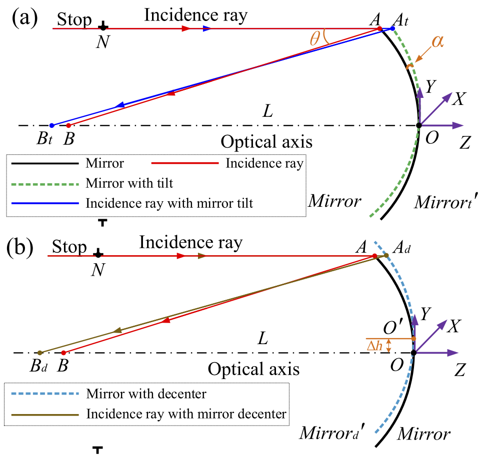

Fig. 1. Mathematical analysis model of the error sensitivity of the single mirror reflective optical system: (a) mirror with tilt, and (b) mirror with decenter.

Analyzing the mirror applied at the decenter error, ΔWE can be expressed as

$$\begin{aligned}\Delta WE &= (NA_d + A_dB_d) - (NA + AB) \\ &= AA_d + A_dB_d - AB.\end{aligned} \quad \textbf{(1)}$$

To simplify the calculation, the ellipsoidal surface type of the mirror is chosen, that is, the conic coefficient $k = -1$. Using the center of the mirror point O as the coordinate origin to establish the Cartesian coordinate system, the mirror equation can be expressed as follows:

$$z = 1/2cr^2 (z<0), \quad \textbf{(2)}$$

where z is the sag of the surface parallel to the optical axis, c is the curvature of the surface, and r is the radial distance.

Since the conic surface has rotational symmetry, the YOZ plane is chosen for the analysis and the mirror expression can be simplified as

$$z = 1/2cy^2 \quad (z<0). \quad \textbf{(3)}$$

The length of AB can be calculated as

$$AB = \sqrt{h^2 + (L - 1/2ch^2)^2}. \quad \textbf{(4)}$$

According to the amount of decenter error Δh, the mirror expression after applying the error can be obtained as

$$z = 1/2c(y - \Delta h)^2 \quad (z<0). \quad \textbf{(5)}$$

Thus, the coordinates of the point A_d, and the length of AA_d can be calculated as

$$AA_d = 1/2ch^2 - 1/2c(h - \Delta h)^2. \quad \textbf{(6)}$$

Next, make a vertical line through the point A_d to the optical axis to intersect the optical axis at the point C_d, and make a parallel line through the point O' to intersect A_dB_d with the point B_d' and intersect A_dC_d at the point C_d', and make a line parallel to the optical axis through the center O' of the mirror applied the decenter to intersect A_dC_d at the point C_d' and intersect A_dB_d at the point B_d', as shown in Fig. 2.

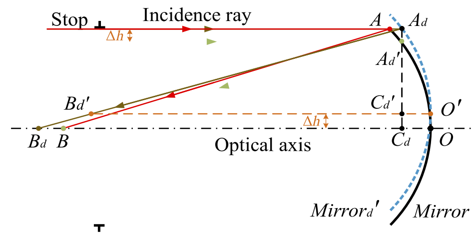

Fig. 2. Auxiliary line diagram of the mirror with decenter.

From the properties of similar triangles, it follows that

$$A_dB_d'/(h - \Delta h) = A_dB_d/h. \quad \textbf{(7)}$$

To solve for the length of A_dB_d', the decenter error is applied to the incidence ray, which means, analyzing the ray with an incidence height of h–Δh, which intersects the mirror at the point A_d':

$$A_d'B = \sqrt{(h - \Delta h)^2 + (L - 1/2c(h - \Delta h)^2)^2}. \quad \textbf{(8)}$$

The decenter error of the mirror is converted over the incidence ray for analysis, avoiding the complex ray tracing of the mirror with the error and cleverly obtaining the length of the reflected ray. What is more, no error arises in this process.

$$A_dB_d' = A_d'B. \quad \textbf{(9)}$$

Taking Eqs. (8) and (9) into Eq. (7), this gives

$$A_dB_d = \frac{h}{h - \Delta h}\sqrt{(h - \Delta h)^2 + (L - 1/2c(h - \Delta h)^2)^2}. \quad \textbf{(10)}$$

Taking Eqs. (4), (6), and (10) into Eq. (1), we obtain

$$\begin{aligned}\Delta WE = c\Delta h(h - 1/2\Delta h) + \sqrt{h^2 + \left(\left(\tfrac{hL}{h-\Delta h}\right)^2 - 1/2ch^2\right)^2} \\ -\sqrt{h^2 + (L^2 - 1/2ch^2)^2}.\end{aligned} \quad \textbf{(11)}$$

When the incidence height h, the decenter error Δh, and the work distance L from the mirror to the image plane are all constant, the smaller the curvature c of the mirror, the smaller the $\Delta WE_{\text{decenter}}$, which means the decenter error sensitivity is lower.

For the tilt error, similar to the decenter error analysis method, when the tilt error is applied to the mirror, the ΔWE_{tilt} is

$$\Delta WE_{\text{tilt}} = AA_t + A_tB_t - AB. \quad \textbf{(12)}$$

The same ray shift with error method is used for the analysis, as shown in Fig. 3, where a vertical line is made across point O in the positive direction of the y axis to intersect the extension of the incidence ray at point D. The extension of the incidence ray

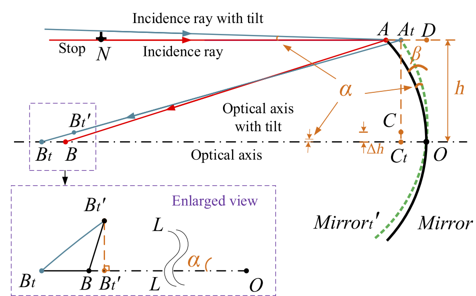

Fig. 3. Auxiliary line diagram of the mirror with tilt.

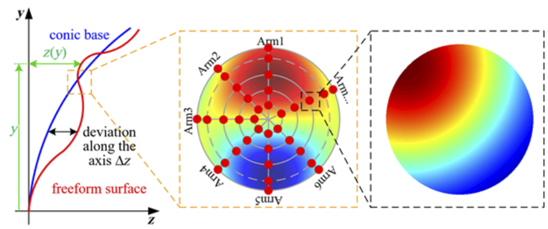

Fig. 4. Schematic diagram of the local small region of freeform surface based on differentiation and ray sampling.

NA intersects the mirror with tilt at point A_t. The incidence ray with tilt and the reflected ray are shown in aqua green, and an optical axis with tilt angle α is drawn, intersecting the reflected ray A_tB_t with point B_t', and the vertical line of the optical axis is made through the point B_t' to intersect the optical axis with the point $B_\perp$, and the geometric relationship between the reflected ray and the intersection of the optical axis is enlarged in the purple box.

Due to the small tilt angle, AA_t can be expressed as

$$AA_t = h\tan(\alpha+\beta) - h\tan\beta \approx h\tan\alpha. \quad (13)$$

The vertical line of the optical axis is made through A_t to intersect the optical axis at the point C_t, and the parallel line of the optical axis is made through the point B_t' to intersect A_tC_t at the point C.

According to the triangle similarity theorem, it is found that

$$\begin{cases} A_tB_t'/A_tC = A_tB_t/A_tC_t, \\ A_tB_t'/(h-\Delta h) = A_tB_t/h. \end{cases} \quad (14)$$

The simplification gives:

$$A_tB_t = h\sqrt{(h-L\sin\alpha)^2 + (L\cos\alpha)^2}/(h-L\sin\alpha). \quad (15)$$

Taking Eqs. (4), (13) and (15) into Eq. (12) we obtain

$$\Delta WE_{\text{tilt}} = h\sqrt{(h-L\sin\alpha)^2+(L\cos\alpha)^2}/(h-L\sin\alpha) - \sqrt{h^2+(L-1/2ch^2)^2} + h\tan\alpha. \quad (16)$$

When the incidence height h, the tilt error angle α, and the distance L from the mirror to the image plane are all constant, the smaller the curvature c of the mirror, the smaller the ΔWE_{tilt}, which means the tilt sensitivity is lower.

In summary, for reflective optical systems, the smaller the curvature of the mirror, the smaller the image quality degradation of the optical system when the mirror is disturbed by errors.

Freeform surface representation is very complex and has no rotational symmetry, but the representation describing a freeform surface must be continuous. Therefore, no matter how complex a freeform surface descriptive equation is, it can be divided into multiple small local regions of conic surfaces by sampling enough points. So, this Letter proposes a desensitization design method based on *LC* control. By differentiation, the freeform surface is divided into several small regions, each of which can be regarded as a small conic surface, as shown in Fig. 4. The overall desensitization is achieved by reducing the error sensitivity of each small region.

Using the "Ring-Arm" pupil sampling method, *NOR***NOA* reference points are selected, and the error sensitivity evaluation function is constructed by calculating the *LC* of a small area around each reference point, which is divided into two steps.

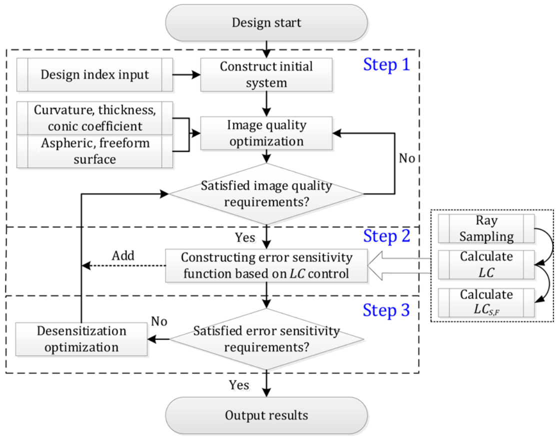

Fig. 5. Flow chart of the desensitization design method for freeform optical systems based on *LC* control.

According to the "Ring-Arm" sampling method, the error sensitivity of a freeform surface for an FOV point is expressed as

$$LC = \sqrt{\frac{\sum_{u=1}^{NOR}\sum_{v=1}^{NOA} LC_{u,v}^2}{NOR \cdot NOA}}, \quad (17)$$

where *NOR* is the number of the Ring, u is the serial number of the Ring. *NOA* is the number of the Arm, and v is the serial number of the Arm.

The error sensitivity of the optical system for all FOV points is expressed as

$$LC_{S,F} = \frac{\sum_{k=1}^{NOF}\sqrt{\sum_{i=1}^{NOS}\frac{LC_i^2}{NOS}}}{NOF}, \quad (18)$$

where *NOS* is the number of the Surface, n is the serial number of the Surface, *NOF* is the number of the FOV point, and m is the serial number of the FOV point.

Based on the above analysis, we propose a desensitization design method based on *LC* control. The method can be divided into the following steps, and the flow chart is shown in Fig. 5.

(1) Image quality optimization and evaluation. In the optimization process, the curvature, thickness, conic coefficients, and high-order term coefficients of the mirror are set as optimization variables. In order to achieve better image quality, the surface type can be gradually upgraded from spherical, to aspheric, to freeform surfaces.
(2) Construction of error sensitivity evaluation function. The error sensitivity evaluation function is constructed according to the number of elements in the optical system and the complexity of the surface type.
(3) Error sensitivity evaluation and optimization. The error sensitivity of the optical system is evaluated, and if the error sensitivity requirement is met, the system can be output as the final result; if not, the optical system needs to be optimized until the optical system meets the requirements of both the image quality and error sensitivity.

An off-axis three-mirror optical system with a focal length of 850 mm, *F*#4.25, an FOV of 20°×30°, and working at 588 nm is

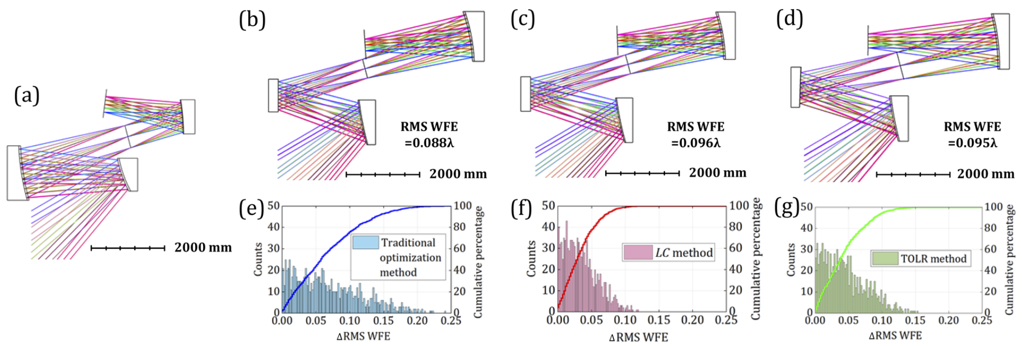

Fig. 6. Optical systems layout of (a) initial structure, (b) "System 1", (c) "System 2", and (d) "System 3"; Monte Carlo tolerance analysis results of the optical system obtained by (e) traditional optimization method, (f) our proposed *LC* method, and (g) TOLR method.

Table 1. Comparison of Three Optimization Methods

	System 1 (Only WFE)	System 2 (*LC*)	System 3 (TOLR)
Optimize time	4–5mins	≈10mins	18 hours
$LC_{S,F}$	0.638	0.400	0.625
Nominal value/λ	0.088	0.096	0.095
ΔRMS WFE average value/λ	0.068	0.034	0.054

used as an example to validate the proposed method. The layout of initial structure is shown in Fig. 6(a).

In this example, the surface type of the three mirrors is upgraded to *XY* polynomial freeform surface, using the first to seventh order terms. The traditional optimization method is used to obtain an optical system with good image quality, named "System 1," and the wavefront error (WFE) of "System 1" is 0.088λ. The layout is shown in Fig. 6(b). The allowable range of image quality in desensitization process is set as 0.088λ±10%.

Since the optical system FOV is large and the optical system does not have rotational symmetry, 35 FOV points (X: –15°, –10°, –5°, 0°, 5°, 10°, 15°; Y: 30°, 35°, 40°, 45°, 50°) are selected. The pupil sampling method corresponding to each FOV point is 8 Rings and 10 Arms, which means that one pupil is divided into 80 small areas. The desensitization design method mentioned above is used to optimize "System 1." After ten minutes of optimization, the optimized system is named "System 2." The WFE of "System 2" is 0.096λ, and the layout is shown in Fig. 6(c). The CPU used in the optimization is an Intel Core I5-9400F @2.90 GHz.

As a comparison, "System 1" was desensitized and optimized by the TOLR method (Zemax built-in). After 18 hours, the optimized result was obtained, named "System 3." The WFE of "System 3" is 0.095λ, and the layout is shown in Fig. 6(d).

Now we will compare the as-built performance of these three systems. We used the Monte Carlo tolerance analysis method with 2000 samples to predict the as-built performance. The error is tilt 0.01° and decenter 0.01 mm, and focus compensation is used. The ΔRMS WFE average values of 2000 Monte Carlo samples are analyzed. The statistical results are shown in Figs. 6(e)–6(g) and Table 1. The image quality degradation of the desensitized optimized optical system is about 9%. However, the results of Monte Carlo analysis show that the as-built performance of the traditional optimization method is seriously degraded. The ΔRMS WFE average value of the optical system optimized by our method is 50% of the original one under the same error conditions. In terms of optimization time, our method can complete the optimization within ten minutes, while Zemax's TOLR method requires at least 18 hours; what's more, the system designed by our method performs better in Monte Carlo analysis.

In this Letter, a design method for evaluating and optimizing the error sensitivity of freeform surface optical systems is proposed. This method can be used together with the image quality optimization. The optimization example and Monte Carlo tolerance analysis show that, although the nominal value of system WFE of the *LC* optimization method is 0.008λ larger than that of the traditional method, the Monte Carlo tolerance sample's ΔRMS WFE average value is 0.034λ smaller than that of the traditional method. In addition, we compared our method with Zemax's built-in TOLR method and found that the optimization efficiency of our method is much better than the TOLR method. Although the desensitization optimization sacrifices a little image quality, it greatly improves the ability of the optical system to resist error interference. We think this process is of great significance.

Funding. Youth Innovation Promotion Association of the Chinese Academy of Sciences (2019219); CAS Project for Young Scientists in Basic Research (YSBR-066); National Natural Science Foundation of China (61705220).

Disclosures. The authors declare no conflicts of interest.

Data availability. Data underlying the results presented in this paper are not publicly available at this time but may be obtained from the authors upon reasonable request.

REFERENCES

1. K. Fuerschbach, G. E. Davis, K. P. Thompson, and J. P. Rolland, Opt. Lett. **39**, 2896 (2014).
2. R. A. Hicks, Opt. Lett. **33**, 1672 (2008).
3. J. Reimers, A. Bauer, K.P. Thompson, and J.P. Rolland, Light Sci. Appl. **6**, e17026 (2017).
4. R. Wu, L. Yang, Z. Ding, L. Zhao, D. Wang, K. Li, F. Wu, Y. Li, Z. Zheng, and X. Liu, Opt. Lett. **44**, 2887 (2019).
5. R. Wu, Z. Feng, Z. Zheng, R. Liang, P. Benítez, J. C. Minano, and F. Duerr, Laser Photonics Rev. **12**, 1700310 (2018).
6. B. Zhang, G. Jin, and J. Zhu, Light: Sci. Appl. **10**, 65 (2021).
7. J. P. Rolland, M. A. Davies, T. J. Suleski, C. Evans, A. Bauer, J. C. Lambropoulos, and K. Falaggis, Optica **8**, 161 (2021).
8. J. Sasian, Appl. Opt. **61**, ED3 (2022).
9. J.P. McGuire, Proc. SPIE **6342**, 63420O (2006).
10. X. Liu, T. Gong, G. Jin F, and J. Zhu, Opt. Express **26**, 21 (2018).
11. Z. Qin, Y. Qi, C. Ren, X. Wang, and Q. Meng, Photonics **9**, 544 (2022).
12. Z. Qin, X. Wang, C. Ren, Y. Qi, and Q. Meng, Opt. Express **29**, 26 (2021).